Light scattering and absorption properties of dust particles retrieved from satellite measurements

R.-M. Hu, and R.S. Sokhi,

Centre for Atmospheric and Instrumentation Research (CAIR), University of Hertfordshire, College Lane, Hatfield, AL109AB, UK.

Short title: SATELLITE REMOTE SENSING OF AEROSOLS

Abstract.

We use the radiative transfer model and chemistry transport model to improve our retrievals of dust optical properties from satellite measurements. The optical depth and absorbing optical depth of mineral dust can be obtained from our improved retrieval algorithm. We find the nonsphericity and absorption of dust particles strongly affect the scattering signatures such as phase function and polarization at the ultraviolet wavelengths. From our retrieval results, we find the high levels of dust concentration occurred over most desert regions such as Saharan and Gobi deserts. The dust absorption is found to be sensitive to mineral chemical composition, particularly the fraction of strongly absorbing dust particles. The enhancement of polarization at the scattering angles exceeding 120 degree is found for the nonspherical dust particles. If the polarization is neglected in the radiative transfer calculation, a largest 50 percent of error is introduced for the case of forward scattering and 25 percent of error for the case of backscattering. We suggest that the application of polarimeter at the ultraviolet wavelengths has the great potential to improve the satellite retrievals of dust properties. Using refined optical model and radiative transfer model to calculate the solar radiative forcing of dust aerosols can reduce the uncertainties in aerosol radiative forcing assessment.

1. Introduction

Mineral dust particles are the most widespread natural and anthropogenic aerosols and play an important role in climate forcing by altering the earth's energy budget through the scattering and absorption of radiation (Tegen et al., 1996; Sokolik and Toon, 1996), and changing the cloud formation (Kaufman et al., 2005). In spite of decadal efforts, the detailed information on physical, chemical and optical properties of mineral dust is still limited.

Satellite remote sensors have provided rich information on aerosol optical properties in recent years (King et al., 1999; Mishchenko et al., 1999; Kaufman et al., 2002, Kahn et al., 2005). However, the uncertainties stem from simplified assumptions of dust composition, dust profile, dust mixing state and morphology used in retrieval algorithms. Several studies have demonstrated the significant effect of nonsphericity on aerosol retrieval (Dubovik et al., 2002; Kalashnikova et al., 2005). The theoretical computation of light scattering properties for the realistic nonspherical particles still remains a difficult task and limited for a few particle shapes. Meanwhile, the dust particles are a complicated mixture of various minerals with different optical properties (Sokolik and Toon, 1999). The mixing state of each dust particle depends on the origin of the dust, on mobilization and on the chemical transformation during its transport. Lack of such information leads to the limitation on the retrieval of complex refractive index and size distribution from the satellite measurements.

The Total Ozone Mapping Spectrometer (TOMS) Aerosol Index (AI) was used to detect the dust sources because TOMS AI is sensitive to the absorbing dust particles (Herman et al., 1997; Torres et al., 1998). Aside from the AI, Hsu et al. [2004] retrieved the aerosol properties over bright-reflecting surfaces using measurements from Moderate Resolution Imaging Spectroradiometer (MODIS) and Sea-viewing Wide Field of View Sensor(SeaWiFS). The outstanding issues relevant to dust optical properties include the following: (1) How much does the dust size distribution affect the optical properties? (2) How much can we know about the internal inhomogeneity of dust particles? (3) Is there a robust spectral signal of optical quantities for nonspherical dust particles? (4) Can we extract more optical information of dust particles from satellite measurements? In this study, we use TOMS, MODIS and the Multiangle Imaging SpectroRadiometer (MISR) measurements to retrieve the optical properties of dust particles. The additional information from global chemistry transport model (GEOS-Chem) is used to improve the results of satellite retrievals of dust aerosol optical depth (AOD) and absorbing aerosol optical depth (AAOD). The sensitivity of backscattered radiances measured by satellite sensors to dust properties will be examined.

2. Methodology

The backscattered radiance measured by satellite sensors can be converted to aerosol optical properties such as AOD and aerosol effective radius. In order to estimate the dust AOD, we use the AOD data from the Moderate Resolution Imaging Spectrometer (MODIS) measurements (Chu et al, 2002, Remer et al., 2002). As the data over bright surface such as Saharan desert are removed, we use the Multiangle Imaging Spectro-Radiometer (MISR) (Kahn et al., 2005) AOD data over these regions. The calculation of dust AOD τ_{dust} is as follows:

$$\tau_{dust}(\lambda) = \tau_a(\lambda) f_{dust} \tag{1}$$

Where τ_a is AOD at wavelength λ and f_{dust} is the fraction of dust aerosols. We use the aerosol fraction values generated from GEOS-Chem model (Bey et al., 2001, Park et al., 2005). The model is driven by assimilated meteorological data from the Goddard Earth Observing System (GEOS-3) at the NASA Global Modeling and Assimilation Office (GMAO). The mineral dust simulation is based on the Dust Entrainment and Deposition (DEAD) scheme Zender et al. (2003) as implemented by Fairlie et al. [2006]. The size distribution of dust aerosols is assumed to be lognormals with four size bins (Martin et al., 2003).

For dust aerosol absorption, we first retrieve the column effective aerosol single scattering albedo (ω_0) that reproduces the Total Ozone Mapping Spectrometer (TOMS) or the current Ozone Monitoring Indtrument (OMI) Aerosol Index (AI)(Torres et al., 2005), when constrained by MODIS and MISR aerosol optical depth and by relative vertical profiles from GEOS-Chem model (Hu et al., 2007). The

Single Scattering Albedo (SSA), nonspherical fraction from MISR, coarse aerosol fraction from MODIS, and AOD or absorbing AOD at the ultraviolet wavelengths from OMI are currently available. We use a Mie scattering algorithm (Mie, 1908) for small spherical dust particles and the T-Matrix algorithm (Mishchenko et al., 1995) for large non-spherical dust particles to calculate the optical quantities. Table 1 presents the imaginary refractive indices of dust particles dependent on the chemical compositions such as Hematite or Quartz (Sokolik and Toon, 1999). We select different mixing types of dust particles which are Quartz mixed with 1 percent or 10 percent of Hematite. We use modified Extended Effective Medium Approximations (EEMAs) to calculate the refractive indices of mineral component mixture. Our values are confirmed by the good agreement with other studies (Colarco et al., 2002). The total backscattered radiance is calculated by the vector discrete ordinate radiative transfer model VLIDORT (with polarization) for different dust shapes, sizes and chemical compositions (Spurr, 2007; Natraj etal., 2006). A look-up table of backscattered radiances was developed for a variety of atmospheric and surface conditions as the function of all sun-satellite viewing geometries. The calculated TOMS AI is adjusted by particle number concentration, size and shape to match the observed TOMS AI. The most likely solution is selected by a chi-squared minimization method for ambiguous solutions (Hu et al., 2002). As we assume the external mixing state of aerosol components such as sulfate, soot, mineral dust, sea salt and organics, the dust ω_0 can be calculated from the column effective ω_0 with the aerosol fractions inputted from GEOS-Chem simulations. Then we can calculate the dust absorbing aerosol optical depth (AAOD) from the dust AOD and ω_0. For the wavelength dependence of AOD, we use Angstrom exponents to convert the dust optical depth at one wavelength to those at other wavelengths.

Finally, the instantaneous solar radiative forcing of dust particles at the top of atmosphere can be calculated using radiative transfer model LIDORT, with 16 wavebands and 16 streams. The surface albedo is adjusted for different wavebands based on the TOMS retrievals in the ultraviolet spectra (Herman et al., 1997) and MODIS retrievals in the visible and near-infrared spectra (Schaaf et al., 2002). The solar radiative fluxes at 16 wavebands are calculated over the solar zenith angles as the function of latitude and time, then integrated to get the instantaneous solar radiative forcing.

3. Results

The vertical profiles of dust particles are determined from the GEOS-Chem simulations. We performed dust simulation for the year 2003. Figure 1 presents the vertical profiles of dust particles for different size bin at Dahkla, Western Sahara. We find that the dust particles can be lifted to high level under the suitable meteorological condition. Interestingly, the peak altitudes of dust profiles for particle radius between 0.1 and 3 μm are almost same.

Figure 2 illustrates the impact of particle shape and composition on the phase function at 360 nm. The spheroid with aspect ratio of 1.5 is used to calculate the scattering properties of randomly oriented nonspherical particles. The lognormal size distribution of dust particles is applied with the mean radius of 0.5 μm and the standard deviation of 2.0. We find the distinct scattering signatures of nonspherical particles from spherical particles when the scattering angle exceeds 120 degree. The mixtures of strong absorbing dust particles such as Hematite can greatly change the scattering properties for the large scattering angles. Similar features are also found for the degree of linear polarization (Figure 3). It is interesting to find the enhancement of polarization for the strongly absorbing particles at the scattering angle of around 50 degree. This distinct signature is very special for the ultraviolet wavelengths. we suggest that the potential application of high-precision polarization in the ultraviolet radiance measurements can increase the capability of detecting dust sources.

Figure 4 shows the dust aerosol radiances calculated by using VLIDORT with polarzation and LIDORT without polarization. We find that neglecting polarization in the radiative transfer calculation causes errors in the calculated radiances. The errors increase rapidly with scattering angle between 0 degree and 90 degrees. A largest error 50 percent is introduced for the case of forward scattering and 25 percent error for the case of backscattering. Generally, the greater polarization induces greater error. For this reason, it is important to understand the effect of neglecting polarization on dust aerosol retrievals.

Figure 5 presents the TOMS AI contributed from only dust particles. We use the polarized radiative transfer model to calculate the radiances at 331 nm and 360 nm. The large values of TOMS

AI occurred over most desert areas. The polarization effect on the calculation of TOMS AI is shown in Figure 6. We find the error due to polarization effect increases as the dust particles loading increases. The intensity increases due to greater scattering while the polarization decreases. Increasing the aerosol loading leads to an increase of the total optical depth and causes more multiple scattering.

Figure 7 shows the dust AOD at 360 nm retrieved from MODIS and MISR during spring of 2003. The high values of AOD are seen over Sahara, Gobi and Australia deserts with strong dust emission sources. The enhancement of AOD over the part of Atlantic Ocean, East Asia, Pacific Ocean and North America is the clear evidence that dust particles are long range transported far away from source regions. The high levels of dust concentration over the Atlantic Ocean in the downwind of Saharan region are consistent with previous studies (Prospero et al., 2002). The dust particles originated from the seasonal dust storms are harmful to human health and create poor visibility in surrounding regions.

Figure 8 presents the dust AAOD derived from dust AOD and ω_0. High values of AAOD are found over areas driven by dust storms. As the AAOD is less sensitive to cloud contamination and aerosol humidification (Kaufman et al., 2006), it is very suitable to detect aerosol type such as dust particles. The high values of dust AAOD have been found over the Atlantic Ocean in the downwind of Saharan region. Considering the AAOD sensitive to the imaginary refractive indices, we use the external and internal mixing approach to decide the imaginary refractive index values. However the values of imaginary refractive indices of mineral dust vary widely among literature surveys. The difficulty of setting correctly the values of the imaginary refractive indices is related to the uncertainty of dust component fraction. Furthermore, the dust particles have also been observed to be mixed with other absorbing aerosols such as black carbon or brown carbon (Liu and Mishchenko, 2007). This can lead to the excessive absorption of mineral dust. More in situ measurements of dust chemical composition and mixing state are crucial to reduce the uncertainty in the dust absorption estimation.

Figure 9 presents the instantaneous solar radiative forcing at the top of atmosphere. The figure shows the mean values of solar radiative forcing during spring of 2003. We find strong negative solar radiative forcing occurred over the most parts of deserts and near areas, particularly over Saharan desert. The values are consistent with the measurements conducted over Saharan region (Haywood et al., 2003). We realize that the solar radiative forcing calculation of dust particles from refined optical model, chemistry transport model and radiative transfer model can reduce the uncertainty in radiative forcing assessment.

The physical and chemical processes of dust formation, evolution and transport are very complicated and this poses considerable challenges for model simulation and satellite retrieval. Uncertainties exist in size distribution, refractive indices, morphology and mixing state of dust particles. Indeed, there is no consensus on the radiative forcing of anthropogenic dust particles in the current stage. Subsequent measurements from the ground-based, airborne and space-based instruments can provide more information on the optical, microphysical, chemical properties, and the temporal and spatial variation of dust particles. The combination of modeling and observation to improve our understanding of dust properties is highly recommended.

4. Conclusions

Retrieval of dust properties over bright surface using satellite measurements at the visible wavelengths such as MODIS is difficult task since the aerosol signal in apparent reflectance is diminished over the bright surface. Although the UV measurements such as TOMS provide the valuable information on the distribution of dust sources, TOMS AI is very sensitive to the altitude of dust loading. In order to improve satellite retrievals, we synergistically use satellite measurements such as MODIS, MISR and TOMS at the ultraviolet and visible channels to retrieve dust properties over the bright surface. The additional information of vertical profiles generated from GEOS-Chem is used to constrain the retrieval uncertainty. The AOD and AAOD of dust particles have been retrieved from such algorithm.

From the analysis of light scattering properties of dust particles, we find the enhancement of backscattering and polarization for nonspherical particles when the scattering angles exceed 120 degree. The distinct signature of phase function and polarization of nonspherical dust particles at the ultraviolet wavelengths is suggested to be great benefit for the implement of polarimeter at the ultraviolet wavelengths. We find the high level of dust concentration occurred in the downwind of Saharan region over the Atlantic Ocean. The dust scattering and absorption properties strongly depend on the chemical composition of dust particles. The fraction of Hematite inside the dust particles is very important to decide the imaginary refractive indices of mineral dust mixtures accurately. Furthermore, the exact information of dust particles mixed with other kind of absorbing aerosols such as black carbon or brown carbon are crucial for the retrieval of dust optical properties. The refined optical model, chemistry transport model and radiative transfer model can be helpful to reduce the uncertainty of aerosol radiative forcing assessment.

Acknowledgments.

We would like to thank Robert Spurr of RT Solutions, Inc. for the use of his VLIDORT radiative transfer model, Michael Mishchenko for the use of his T-Matrix code, and Joseph Ulanowski for the valuable discussion. This work is supported by U.K. Natural Environment Research Council as part of Mesoscale Modelling for Air Pollution Application Network (MESONET) project and the U.K. Environment Agency of Comparison of Simple and Advanced Regional Models (CREMO) project. This work is also funded by grant NE/G007268/1 from the U.K. Natural Environment Research Council.

References

Bey I., D. J. Jacob, J. A. Logan, R. M. Yantosca, Asian chemical outflow to the Pacific: origins, pathways and budgets, *J. Geophys. Res., 106*, 23,097-23,114, 2001.

Chu, D.A., Y.J. Kaufman, C. Ichoku, L.A. Remer, D. Tanre, and B.N. Holben, Validation of MODIS aerosol optical depth retrieval over land, *Geophys. Res. Lett., 29*, 10.1029/2001GL013205, 2002.

Colarco, P.R., O.B. Toon, O. Torres, and P.J. Rasch, Determining the ultraviolet imaginary index of refraction of Saharan dust particles from Total Ozone Mapping Spectrometer data using a three-dimensional model of dust transport, *J. Geophys. Res., 107*, 10.1029/2001JD000903, 2002.

Dubovik, O., B.N. Holben, T.F. Eck, A. Smirnov, Y.J. Kaufman, D. Tanre, and I. Slutsker, Variability of absorption and optical properties of key aerosol types observed in worldwide locations, *J. Atmos. Sci., 59*, 590-608, 2002.

Fairlie, T. D., D. J. Jacob and R. J. Park, The impact of transpacific transport of mineral dust in the United States, *submitted to Atmos. Environ.*, 2006.

Herman, J.R., P.K. Bhartia, O. Torres, C. Hsu, C. Seftor, and E. Celarier, Global distribution of ultraviolet-absorbing aerosols from Nimbus 7-TOMS data, *J. Geophys. Res., 102*, 16911-16922, 1997.

Haywood, J., et al., Radiative properties and direct radiative effect of Saharan dust measured by the C-130 aircraft during SHADE: 1. Solar spectrum, *J. Geophys. Res., 108(D18)*, 8577, doi:10.1029/ 2002JD002687, 2003.

Hsu, N.C., S.C. Tsay, M.D. King, and J.R. Herman, Aerosol properties over bright-reflecting source regions, *IEEE Trans. Geosci. Remote Sens., 42(3)*, 557-569, 2004.

Hu, R.-M., and R.S. Sokhi, Oceanic phytoplankton, atmospheric aerosol and Raman scattering impacts on space-based ultraviolet radiance Measurements, *Atmos. Chem. Phys. Discuss., 7*, 1435114367, 2007

Hu, R.-M., R.V., Martin, and T. D. Fairlie, Global retrieval of columnar aerosol single scattering albedo from space-based observations, *J. Geophys. Res., 112*, D02204, doi:10.1029/2005JD006832, 2007.

Hu, R.-M., K.S. Carslaw, C. Hostetler, L.R. Poole, B. Luo, T. Peter, S. Fueglistaler, T.J. McGee, and J.F. Burris, Microphysical properties of wave polar stratospheric clouds retrieved from lidar measurements during SOLVE/THESEO 2000, *J. Geophys. Res., 107*, 8294, doi:10.1029/2001JD001125, 2002.

Kalashnikova, O. V., R. Kahn, I. N. Sokolik, and W.-H. Li, Ability of multiangle remote sensing observations to identify and distinguish mineral dust types: Optical models and retrievals of optically thick plumes, *J. Geophys. Res., 110*, D18S14, doi:10.1029/2004JD004550, 2005.

Kahn, R., et al., Multiangle Imaging Spectroradiometer (MISR) global aerosol optical depth validation based on 2 years of coincident Aerosol Robotic Network (AERONET) observations *J. Geophys. Res., 110*, D10S04, doi:10.1029/2004JD004706, 2005.

Kaufman, Y.J., D.Tanre, and Boucher, A satellite view of aerosols in the climate system, *Nature, 419*, 215-223, 2002.

Kaufman, Y.J., I. Koren, L. A. Remer, D. Rosenfeld, and Y. Rudich, The effect of smoke, dust and pollution aerosol on shallow cloud development over the Atlantic Ocean, *Proc. Natl. Acad. Sci. U.S.A., 102*, 11207-11212, 2005.

Kaufman, Y.J., I. Koren, Smoke and pollution aerosol effect on cloud cover, *Science, 313*, 655-658, 2006.

King, M.D., et al., Remote sensing of cloud, aerosol and water vapor properties from moderate resolution imaging spectrometer (MODIS), *IEEE Trans. Geosci. Remote.Sens., vol.30*, 2-27, 1992.

Liu, L., and M.I. Mishchenko, Scattering and radiative properties of complex soot and soot-containing aggregate particles. *JQSRT, 106*, 262-273, 2007.

Martin, R.V., D.J. Jacob, R.M. Yantosca, M. Chin, and P. Ginoux, Global and regional decreases in tropospheric oxide emissions constrined by space-based observations of NO2 columns, *J. Geophys. Res., 108*, 4097, doi:10.1029/2002JD002622, 2003.

Mie, G., Beitrage zur Optik truber Medien, speziell Kolloidaler Metallosungen. *Ann. Physik, 25*, 377-445, 1908.

Mishchenko, M. I., and A. A. Lacis, B. E. Charlson, and L. D. Tavis, Nonsphericity of dust-like tropospheric aerosols: Implications for aerosl remote sensing and climate modeling, *Geophys. Res. Lett., 22*, 1077-1080, 1995.

Natraj, V., R. Spurr, H. Boesch, Y. Jiang, and Y. Yung, Evaluation of errors in neglecting polarization in the forward modeling of O2 A band measurements from space, with relevance to CO2 column retrieval from polarization sensitive instruments, *JQSRT*, in press, 2006.

Park, R.J., D.J. Jacob, M. Chin, and R.V. Martin, Sources of carbonaceous aerosols over the United States and implications for natural visibility conditions, *J. Geophys. Res., 108*, 4355, doi:10.1029/2002JD003190, 2003.

Prospero, J. M., P. Ginoux, O. Torres, and S. Nicholson (2002), Environmental characterization of global sources of atmospheric soil dust derived from NIMBUS-7 TOMS absorbing aerosol product, *Rev. Geophys., 3. Summary 40(1)*, 1002, doi:10.1029/2000RG000095.

Remer, L.A., et al., Validation of MODIS aerosol retrieval over ocean, *Geophys. Res. Lett., 29*, doi:10.1029/2001GL013204, 2002.

Schaaf, C. B. et al. First operational BRDF, albedo nadir reflectance products from MODIS. *Remote Sens. Environ. 83*, 135-148, 2002.

Sokolik, I. N., and O. B. Toon, Direct radiative forcing by anthropogenic airborne mineral aerosols, *Nature, 381*, 681-683, 1996.

Sokolik, I. N., O. B. Toon, Incorporation of mineralogical composition into models of the radiative properties of mineral aerosol from UV to IR wavelengths, *J. Geophys. Res., 104(D8)*, 9423-9444, 10.1029/1998JD200048, 1999.

Spurr, R. J. D., VLIDORT: A linearized pseudo-spherical vector discrete ordinate radiative transfer model for forward model and retrieval studies in multilayer, multiple scattering media, *prepare to submit to JQSRT*, 2007.

Tegen, I., A. A. Lacis, and I. Fung, The influence on climate forcing of mineral aerosols from disturbed soils, *Nature, 380*, 419-422, 1996.

Torres, O., P.K. Bhartia, J.R. Herman, Z. Ahmad, and J. Gleason, Derivation of aerosol properties from satellite measurements of backscattered ultraviolet radiation - theoretical basis, *J. Geophys. Res., 103*, 17099-17110, 1998.

Zender C. S., H. Bian, D. Newman, Mineral Dust Entrainment and Deposition (DEAD) model: Description and 1990s dust climatology, *J. Geophys. Res., 108 (D14)*, 4416, doi:10.1029/2002JD002775, 2003.

Received ______________________

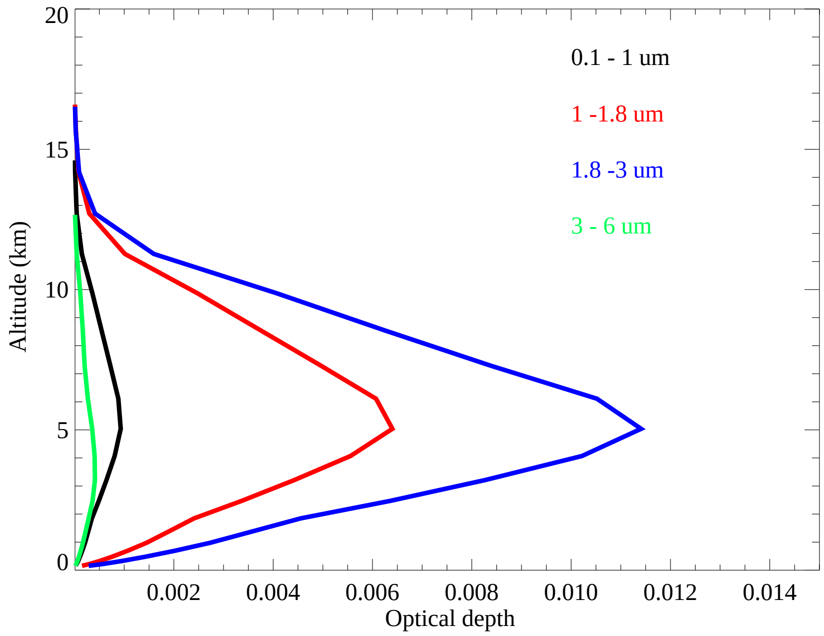

Figure 1. The vertical profiles of dust particles simulated by GEOS-Chem at Dahkla.

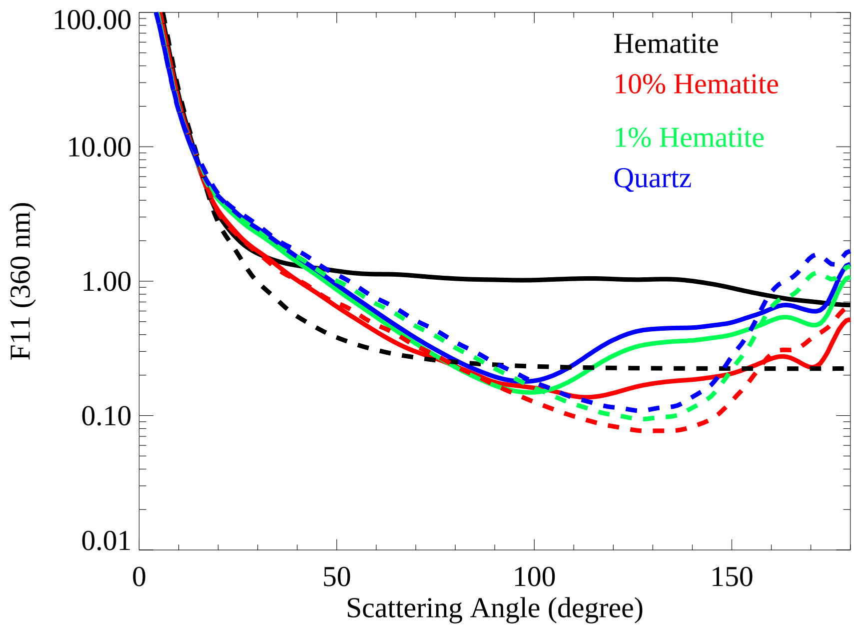

Figure 2. Dust aerosol scattering phase function. Solid lines: T-Matrix calculations for oblate (Mode radius=0.5; aspect ratio=1.5. Dashed lines: Mie theory calculations.

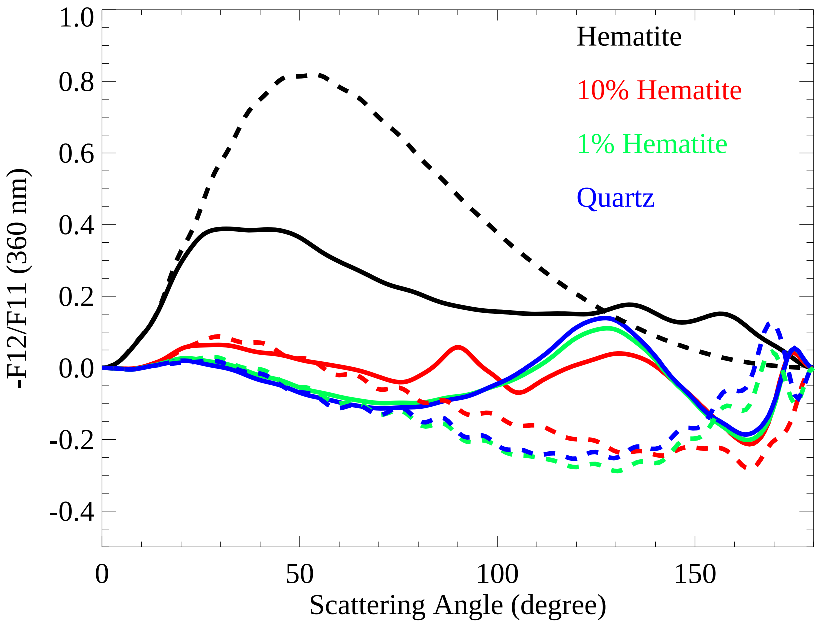

Figure 3. Dust aerosol polarization. Solid lines: T-Matrix calculation for oblate (Mode radius=0.5; aspect ratio=1.5. Dashed lines: Mie theory calculations.

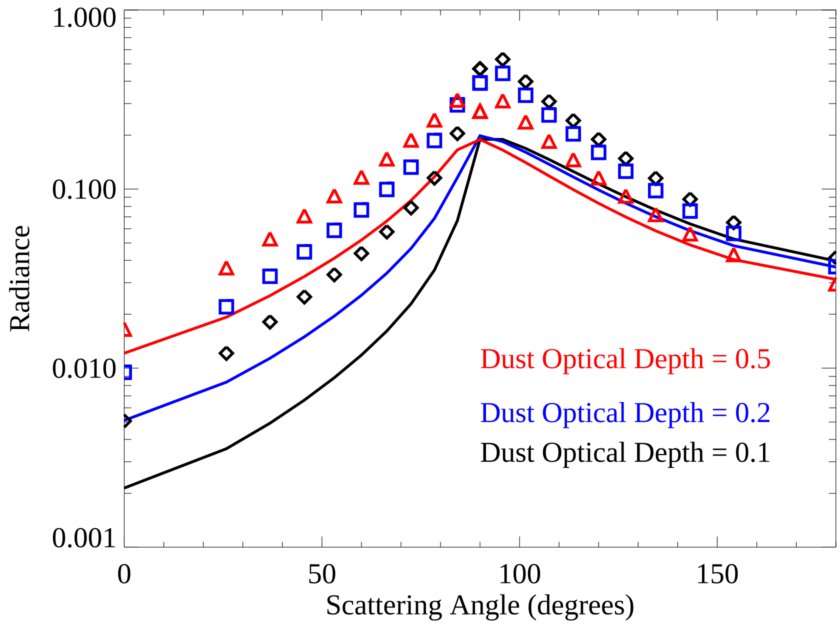

Figure 4. Polarized and unpolarized radiances calculated for dust aerosols at the wavelength of 360 nm. The solar zenith angle, relative azimuth angle and surface reflectivity are 48 degrees, 180 degrees and 0.1, respectively. Symbols denote the polarized randiances and curves denote the unpolarized randiances.

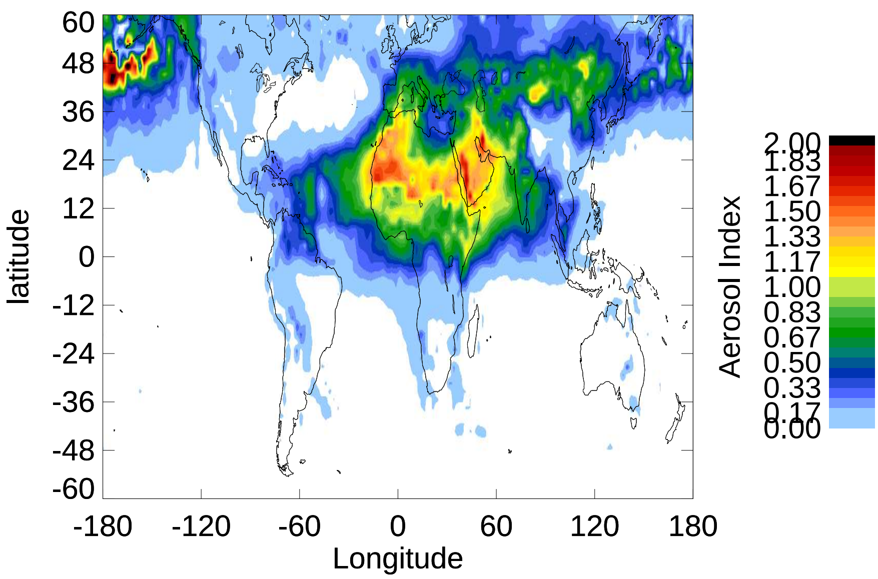

Figure 5. Calculated TOMS Aerosol Index contributed from dust particles.

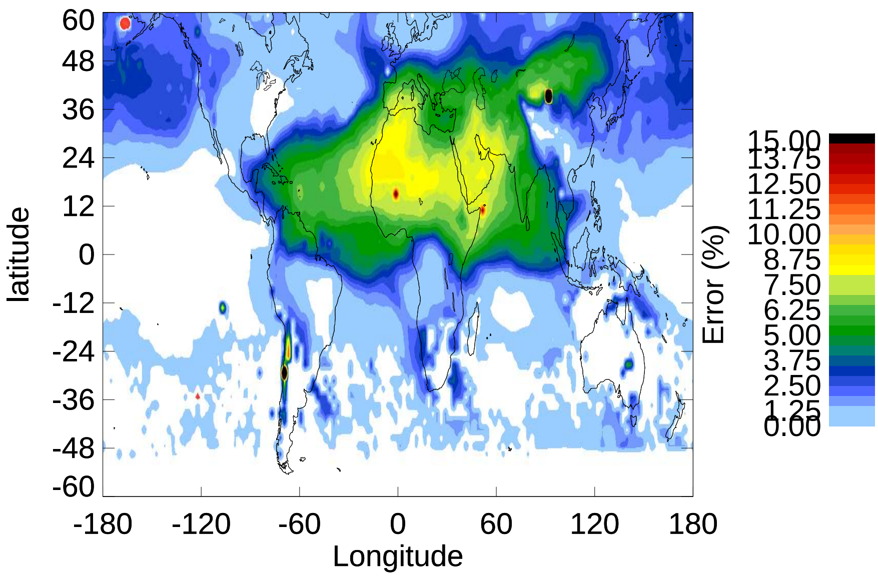

Figure 6. The error of calculated TOMS Aerosol Index if polarization is neglected.

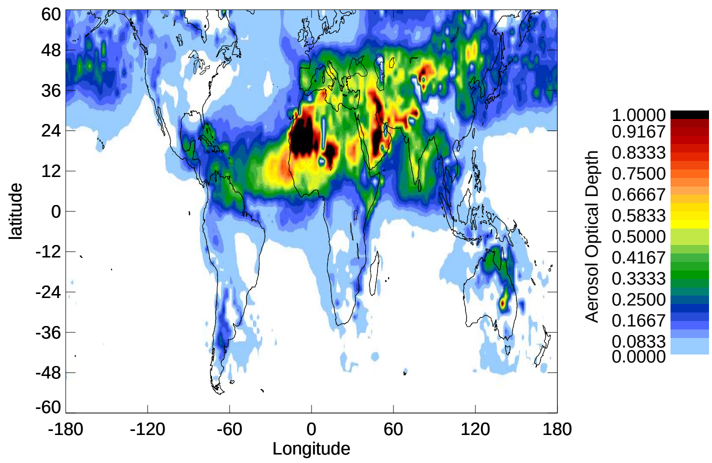

Figure 7. The dust aerosol optical depth retrieved from satellite measurements during spring of 2003.

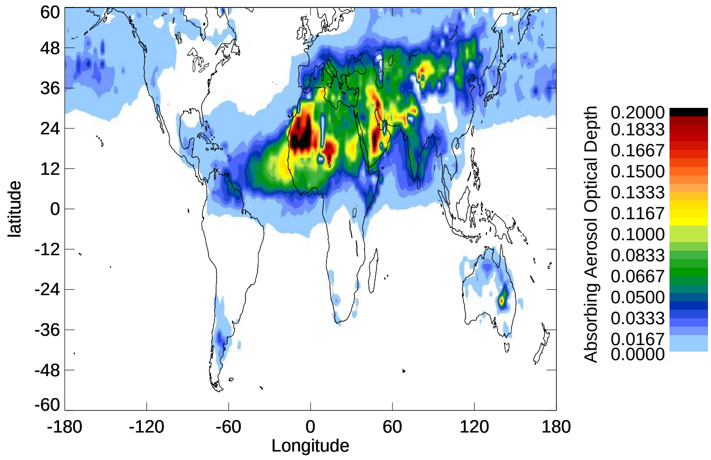

Figure 8. The dust AAOD retrieval from satellite measurements during spring of 2003.

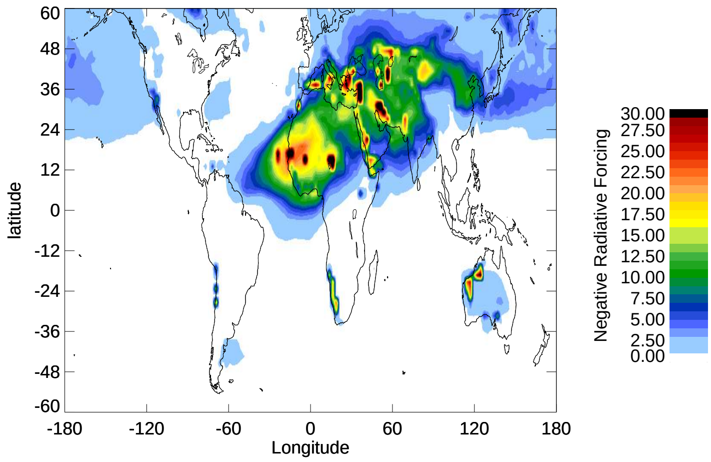

Figure 9. The solar radiative forcing (W/m2) of dust aerosols at TOA calculated from VLIDORT during spring of 2003.

Table 1. Imaginary (mi) refractive indices at 360 nm of minerals

Mineral	mi
Hematite	-1.3
Illite	-0.0017
Kaolinite	-0.0055
Montmorillonite	-0.00035
10 percent Hematite	-0.02
1 percent Hematite	-0.004
Quartz	from -10^{-8} to -10^{-5}
Calcite	from -10^{-8} to -10^{-5}
Gypsum	from -10^{-8} to -10^{-5}